



**AALBORG UNIVERSITY**  
DENMARK

**Aalborg Universitet**

**Mathematical modeling and experimental study of biomass combustion in a thermal 108 MW grate-fired boiler**

Yin, Chungeng; Rosendahl, Lasse Aistrup; Kær, Søren Knudsen; Clausen, Sønnik; L. Hvid, Søren; Hille, Torben

*Published in:*  
Energy & Fuels

*DOI (link to publication from Publisher):*  
[10.1021/ef700689r](https://doi.org/10.1021/ef700689r)

*Publication date:*  
2008

*Document Version*  
Publisher's PDF, also known as Version of record

[Link to publication from Aalborg University](#)

*Citation for published version (APA):*

Yin, C., Rosendahl, L., Kær, S. K., Clausen, S., L. Hvid, S., & Hille, T. (2008). Mathematical modeling and experimental study of biomass combustion in a thermal 108 MW grate-fired boiler. *Energy & Fuels*, 22(2), 1380-1390. DOI: 10.1021/ef700689r

**General rights**

Copyright and moral rights for the publications made accessible in the public portal are retained by the authors and/or other copyright owners and it is a condition of accessing publications that users recognise and abide by the legal requirements associated with these rights.

- ? Users may download and print one copy of any publication from the public portal for the purpose of private study or research.
- ? You may not further distribute the material or use it for any profit-making activity or commercial gain
- ? You may freely distribute the URL identifying the publication in the public portal ?

**Take down policy**

If you believe that this document breaches copyright please contact us at [vbn@aub.aau.dk](mailto:vbn@aub.aau.dk) providing details, and we will remove access to the work immediately and investigate your claim.

## Mathematical Modeling and Experimental Study of Biomass Combustion in a Thermal 108 MW Grate-Fired Boiler

Chungen Yin,<sup>\*,†</sup> Lasse Rosendahl,<sup>†</sup> Søren K. Kær,<sup>†</sup> Sønnik Clausen,<sup>‡</sup> Søren L. Hvid,<sup>§</sup> and Torben Hille<sup>§</sup>

*Institute of Energy Technology, Aalborg University, 9220 Aalborg East, Denmark, Risø National Laboratory, Technical University of Denmark, 4000 Roskilde, Denmark, and DONG Energy, Kraftværksvej 53, 7000 Fredericia, Denmark*

*Received November 16, 2007. Revised Manuscript Received January 4, 2008*

Grate boilers are widely used to fire biomass for heat and power production. However, grate-firing systems are often reported to have relatively high unburnout, low efficiency, and high emissions and need to be optimized and modernized. This paper presents the efforts toward a reliable baseline computational fluid dynamics (CFD) model for an industrial biomass-fired grate boiler, which can be used for diagnosis and optimization of the grate boiler as well as the design of new grate boilers. First, on the basis of the design conditions, a thorough sensitivity analysis is done to evaluate the relative importance of different factors in CFD analysis of the grate boiler. In a late stage, a two-day measuring campaign is carried out to measure the gas temperatures and the gas concentrations in the boiler using a fiber optic probe connected to a Fourier transform infrared spectrometer. A baseline model is then defined on the basis of the sensitivity analysis and the measurements. The baseline results show an overall acceptable agreement with the measured data and the site observations, indicating that the baseline model is applicable in the optimization of the boiler and the design of new grate boilers. However, at a few measuring locations larger discrepancies between the baseline results and the measurements are still observed. It is mainly because the boundary conditions used in the baseline model could be different from those in the real boiler. For instance, the noncontinuous biomass feeding and grate movement, the combustion instabilities inside the fuel bed, and the irregular deposit formed on the furnace walls and air nozzles all make it difficult to derive the reliable boundary conditions that the CFD modeling requires. The baseline results and the measured results show the mixing and combustion behavior in the ideal furnace and in the real furnace, respectively. The local discrepancies may quantify the effect of the differences in the boundary conditions used in the baseline model and in the real boiler.

### Introduction

The worldwide concern about global warming because of the emission of CO<sub>2</sub> and other greenhouse gases and the limited availability of fossil fuels has increased the interest in using biomass as a fuel for energy production. Grate-fired systems and fluidized bed combustors are currently the two main competing technologies used to fire biomass alone in large-scale plants for heat and power production, and their main characteristics are well discussed and summarized.<sup>1–3</sup> A grate furnace can be interpreted as a cross-flow reactor, where solid fuel is fed in a thick layer perpendicular to the primary air (PA) flow. The bottom of the fuel bed is exposed to preheated PA while the top of the bed resides within the furnace. As the first combustion system used for solid fuels, grate boilers are often labeled “high unburnout, low efficiency and high emissions”, which makes the optimization very necessary, in both operation and design. Operation conditions affect greatly the performance

of a grate boiler,<sup>4,5</sup> and operation optimization could be the simplest way to improve the performance of the existing grate boilers. The design of new grate-firing systems can also be modernized, for instance, by optimizing the local furnace geometry (e.g., arch, nose, or neck), using advanced air supply systems, and improving the fuel feeding and grate systems. The optimization in operation and design can greatly increase efficiency, lower emissions (e.g., the pollutants as a result of incomplete combustion, NO<sub>x</sub>, and dioxins), and mitigate other related problems (e.g., ash particle carry-over, deposition, and

\* To whom correspondence should be addressed. Telephone: +45 99409279. Fax: +45 98151411. E-mail: chy@iet.aau.dk.

<sup>†</sup> Aalborg University.

<sup>‡</sup> Technical University of Denmark.

<sup>§</sup> DONG Energy.

(1) Goerner, K. *IFRF Combust. J.* **2003**, 1–32; Article No. 200303.

(2) Morrow, R. S. 2005. <http://www.mass.gov/doer/rps/mor-rpt.pdf> (accessed Feb 12, 2008).

(3) Werther, J.; Saenger, M.; Hartge, E. U.; Ogada, T.; Siagi, Z. *Prog. Energy Combust. Sci.* **2000**, 26, 1–27.

(4) Lillieblad, L.; Szpila, A.; Strand, M.; Pagels, J.; Rupa-Gadd, K.; Gudmundsson, A.; Swietlicki, E.; Bohgard, M.; Sanati, M. *Energy Fuels* **2004**, 18, 410–417.

(5) Strand, M. *Energy Fuels* **2007**, 21, 3653–3659.

(6) Alstom Power Inc. *Journal Articles by FLUENT Software Users* **2004**, JA147, 1–5.

(7) Blasiak, W.; Yang, W. H.; Dong, W. *J. Energy Inst.* **2006**, 79, 67–74.

(8) Dong, W.; Blasiak, W. *Energy Convers. Manage.* **2001**, 42, 1887–1896.

(9) Frey, H. H.; Peters, B.; Hunsinger, H.; Vehlow, J. *Waste Manage.* **2003**, 23, 689–701.

(10) Goddard, C. D.; Yang, Y. B.; Goodfellow, J.; Sharifi, V. N.; Swithenbank, J.; Chartier, J.; Mouquet, D.; Kirman, R.; Barlow, D.; Moseley, S. *J. Energy Inst.* **2005**, 78, 106–116.

(11) Goerner, K.; Klasen, T. *Prog. Comput. Fluid Dyn.* **2006**, 6, 225–234.

(12) Griselin, N.; Bai, X. S. *IFRF Combust. J.* 2000; Article No. 200009, pp 1–30.

corrosion) in biomass-fired grate boilers.<sup>2,6–24</sup> Computational fluid dynamics (CFD) modeling is an efficient way to optimize combustion systems. Compared to modeling of suspension combustion systems, CFD modeling of biomass-fired grate furnaces is inherently more difficult because of the complexity of the solid biomass bed on the grate, the turbulent reacting flow in the freeboard, and the intensive interaction between them.

The objective of this paper is to establish a reliable baseline CFD model for a thermal 108 MW (108MW<sub>th</sub>) biomass-fired grate boiler, which can be used for diagnosis and optimization of this boiler and design of new grate boilers. The CFD analysis is based on the commercial code FLUENT. First, a sensitivity analysis is done on the basis of the design conditions of the boiler to evaluate the effects of different factors in CFD modeling of grate boilers. A two-day measuring campaign is carried out in a late stage to measure the local gas temperatures and concentrations as well as the deposit growth, to collect the operating parameters, and to observe the overall mixing and combustion pattern in the boiler. On the basis of the sensitivity analysis and the measurements, a baseline CFD model is finally defined. The baseline results are compared to the measured data and the site observations.

### Sensitivity Analysis of CFD Modeling

The purpose of this section is to evaluate the factors that may be important in modeling of biomass-fired grate boilers. All the simulations in this section are based on the design conditions in the ideal boiler, which could be different from the real conditions during the measuring campaign. On the basis of the sensitivity analysis and the measurement, a baseline CFD model is defined later. Because of the different conditions, the CFD results in this section and in the baseline section are not necessarily comparable.

In this section, the biomass-fired grate boiler under study is introduced first, followed by the modeling methodology used in this paper. Then among all other factors (e.g., inlet diffusion and discretization), the effects of meshes, models for the fuel bed, turbulence, and combustion are highlighted.

**108MW<sub>th</sub> Biomass-Fired Grate Boiler under Study.** The grate boiler, built in 1999 with the designed output of 35 MW electricity and 50 MJ/s heat, is sketched in Figure 1, in which the capital letters (A–L) indicate the measuring ports used in

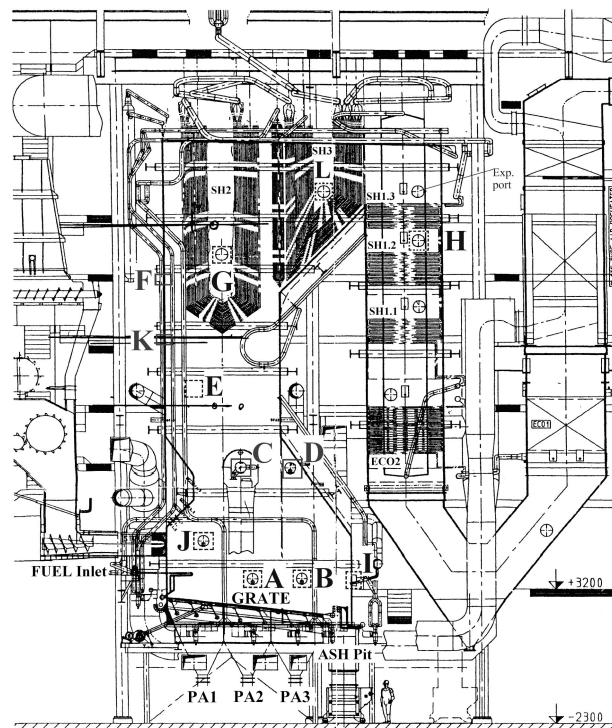


Figure 1. Sketch of the biomass grate-fired boiler and indication of the measuring ports.

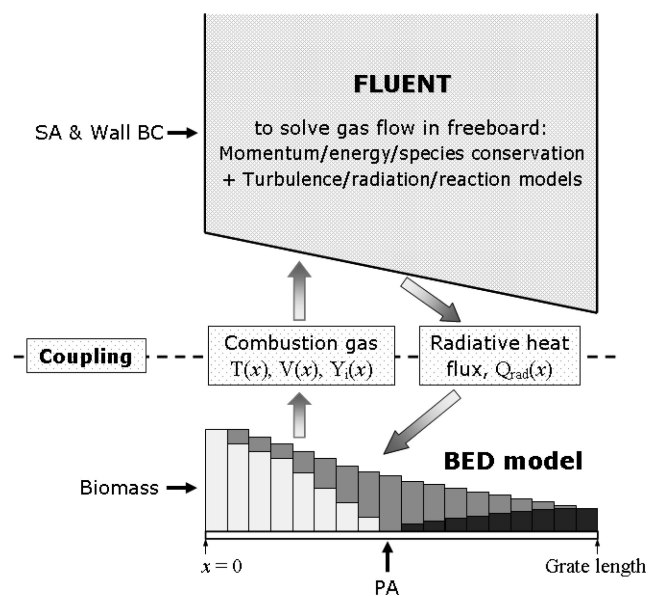


Figure 2. Modeling methodology for biomass-fired grate boilers.

the measuring campaign. See Figure 1s in the Supporting Information for a clearer view of the different processes in this grate boiler.

Four independent water-cooled vibrating grates between the two side walls reside at the bottom in the furnace, exposed directly to the flame and the furnace walls. The grates are made of panel walls with drilled holes in the fins for the PA. The grates are one of the boiler pressure parts, and they are connected to furnace walls by flexible connection pipes which are designed for the vibrations. Four separate feeding lines feed biomass (wheat straw here) into the boiler onto the four grates from the front wall. The grate surface vibrates at high frequency and low amplitudes for about 2% of the time to move the solids forward. As biomass moves forward on the grates, it undergoes a series of conversion processes (i.e., evaporation, pyrolysis, combustion

(13) Huttunen, M.; Kjaldman, L.; Saastamoinen, J. *IFRF Combust. J.* **2004**, 1–8; Article No. 200401.

(14) Kilgroe, J. D. *J. Hazard. Mater.* **1996**, 47, 163–194.

(15) Klason, T.; Bai, X. S. *Prog. Comput. Fluid Dyn.* **2006**, 6, 278–282.

(16) Obernberger, I.; Brunner, T.; Bärnthaler, G. *Biomass Bioenergy* **2006**, 30, 973–982.

(17) Ryu, C. K.; Choi, S. M. *Combust. Sci. Technol.* **1996**, 119, 155–170.

(18) Ryu, C.; Shin, D.; Choi, S. *J. Air Waste Manage. Assoc.* **2002**, 52, 174–185.

(19) Ryu, C.; Yang, Y. B.; Nasserzadeh, V.; Swithenbank, J. *Combust. Sci. Technol.* **2004**, 176, 1891–1907.

(20) Scharler, R.; Obernberger, I.; Längle, G.; Heinze, J. *Proceedings of the 1st World Conference and Exhibition on Biomass for Energy and Industry*, Seville, Spain, June 2000; ETA-Florence: Seville, 2000.





(21) Scharler, R.; Obernberger, I. *Proceedings of 6th European Conference on Industrial Furnaces and Boilers*, Estoril-Lisboa, Portugal, April 2–5, 2002; INFUB: Rio Tinto, 2002; Vol. IV, pp 227–241.

(22) Shanmukharadhy, K. S. *Energy Fuels* **2007**, 21, 1895–1900.

(23) Staiger, B.; Unterberger, S.; Berger, R.; Hein, K. R. G. *Energy* **2005**, 30, 1429–1438.

(24) Walsh, A. R. *Proceedings of the 7th European Conference on Industrial Furnaces and Boilers*, Porto, April 18–21, 2006; INFUB: Rio Tinto, 2006.

Table 1. Two Meshes Used in the Sensitivity Analysis

	Cells: Type, amount and the total amount		EquiAngle skew: Range, percentage, average			
Mesh-I	Hexahedron 	3840295	<b>3840295</b>	$0 \leq Q_{EAS} < 0.25$	84.73%	<b>0.16</b>
	Tetrahedron 	0		$0.25 \leq Q_{EAS} < 0.5$	14.56%	
	Prism 	0		$0.5 \leq Q_{EAS} < 0.73$	0.71%	
	Wedge 	0		$0.73 \leq Q_{EAS} \leq 1$	0	
Mesh-II	Hexahedron	190052	<b>3804598</b>	$0 \leq Q_{EAS} < 0.25$	22.51%	<b>0.35</b>
	Tetrahedron	3506763		$0.25 \leq Q_{EAS} < 0.5$	67.25%	
	Prism	41733		$0.5 \leq Q_{EAS} < 0.75$	9.53%	
	Wedge	66050		$0.75 \leq Q_{EAS} \leq 0.9$	0.71%	

of the released volatiles, and burning of biomass char). Finally, biomass ash is discharged into the ash pit at the end of the grates. To improve the mixing and combustion in the freeboard, totally about 240 secondary air (SA) and overfire air (OFA) nozzles are arranged on the front wall and the rear wall in the boiler.

**Modeling Methodology.** Modeling of a biomass grate-fired boiler involves biomass combustion inside the fuel bed on the grate and gas-phase reactions in the freeboard. The two processes are strongly coupled by the combustion gas leaving the fuel bed into the freeboard and the radiative heat flux emitted by the flame and furnace walls onto the fuel bed, as depicted in Figure 2.

The coupled bed model/CFD approach, as successfully applied elsewhere,<sup>18,25</sup> is used in this study:

Step 1: on the basis of the data of biomass, PA, and incident radiative heat flux, a bed model is solved for the profile of temperature, velocity, and concentrations of combustion gas leaving the fuel bed into the freeboard.

Step 2: CFD modeling of the gas mixing and combustion in the freeboard is carried out, using the output of the bed model as the grate inlet conditions. The CFD solution will give an updated radiative heat flux incident onto the fuel bed.

Step 3: repeat the above two steps until there is no substantial change in either the combustion gas leaving the fuel bed or the radiative heat flux incident onto the fuel layer.

**On Computational Meshes.** The effect of the computational meshes is studied by varying the grid density and the grid

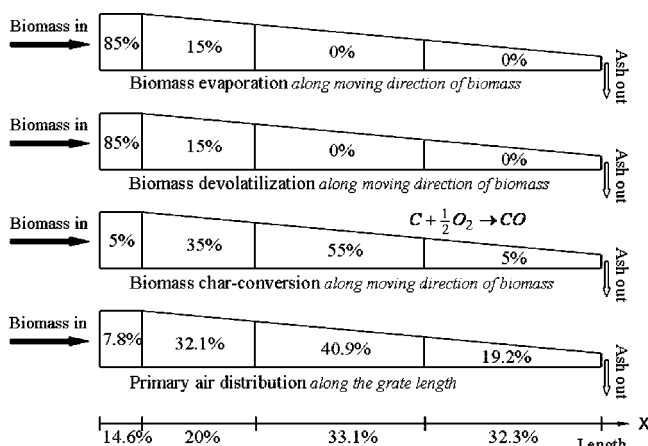


Figure 3. Experience-based conversion rate as a function of position on the grate.

quality. The amount of cells investigated for this boiler varies from about 0.5 M to about 4 M. The two meshes whose results are shown in this paper are as follows:

(1) Mesh-I: It is a pure hexahedron mesh created by dividing the boiler geometry into thousands of individual small sections or volumes, meshing them individually, and then merging the mesh. It is a high-quality mesh that resolves the geometric features quite well and the main flow physics to a reasonable degree of accuracy. The local close-up of the mesh can be seen in Figure 2s in the Supporting Information. Table 1 lists the type and amount of cells, as well as the grid quality report.

(2) Mesh-II: It is a hybrid unstructured tetrahedron-dominant mesh in which local boundary layer and sizing functions are used. It may be the traditional mesh scheme used for the modeling of grate furnaces because such a mesh can be generated in the least amount of time. The type and amount of cells of this mesh, as well as the grid quality, are also shown in Table 1.

Here only the equi-angle skew is given in Table 1, as an example of the grid quality specification. The equi-angle skew represents a normalized measure of skewness, which is defined as follows:

$$Q_{EAS} = \max\left(\frac{\theta_{\max} - \theta_{\text{eq}}}{180 - \theta_{\text{eq}}}, \frac{\theta_{\text{eq}} - \theta_{\min}}{\theta_{\text{eq}}}\right) \quad (1)$$

where  $\theta_{\max}$  and  $\theta_{\min}$  are the maximum and minimum angles (in degrees), respectively, between the edges of the element and  $\theta_{\text{eq}}$  is the characteristic angle corresponding to an equilateral cell of similar form:  $\theta_{\text{eq}} = 60$  for tetrahedral elements and  $\theta_{\text{eq}} = 90$  for hexahedral elements. By definition,  $0 \leq Q_{EAS} \leq 1$ , where  $Q_{EAS} = 0$  describes an equilateral element and  $Q_{EAS} = 1$  describes a completely degenerate (poorly shaped) element.

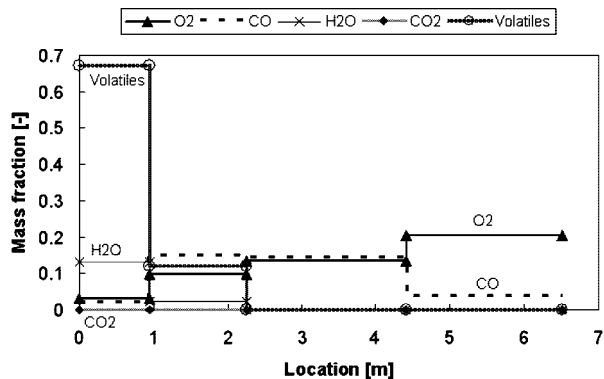
**On Biomass Bed Models.** The fuel bed models play an important role in the modeling of grate boilers because they provide the fuel inlet conditions for the freeboard modeling. Three different approaches on how to treat the fuel bed can be found in literature.

Fluent's porous-media model is used to study the solid-refuse bed on top of a roller grate. The results obtained from this modeling are used as the inlet conditions for the modeling of the freeboard region.<sup>26</sup>

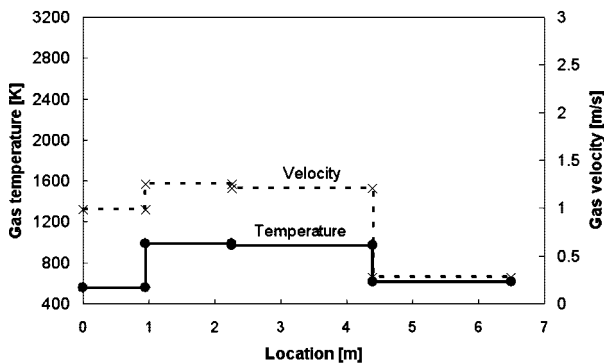
(25) Yang, Y. B.; Newman, R.; Sharifi, V.; Swithenbank, J.; Ariss, J. *Fuel* **2007**, *86*, 129–142.

(26) Nasserzadeh, V.; Swithenbank, J.; Jones, B. *Combust. Sci. Technol.* **1993**, *92*, 389–422.





(a) Gas species at the fuel bed top



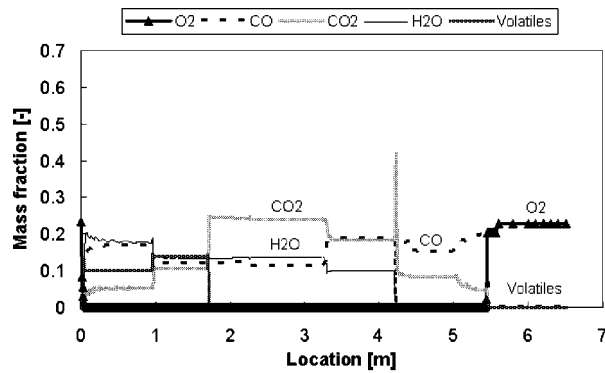
(b) Velocity and temperature at the bed top

Figure 4. Output of Bed Model-I.

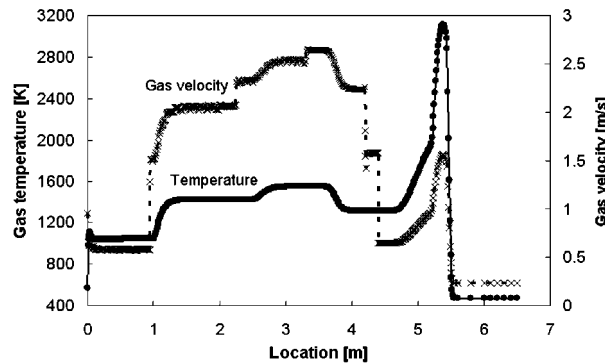
More typically, freeboard modeling treats the fuel bed by using inlet conditions based on experience or measurements. When the combustion rate is prescribed as a function of the position on the grate, inlet conditions (e.g., temperature, velocity, and individual species concentrations) can be calculated from the overall heat and mass balances of the fuel components and the PA.<sup>7,8,11,12,15,20,21,27-29</sup>

Recently, separate bed models have been developed and solved to track the ignition front and the combustion front inside fuel beds, as well as the temperatures, species, and velocity at the fuel bed top: the latter is used as the inlet condition for the freeboard modeling.<sup>10,13,18,19,25,30</sup> Because of the complexity of the fuel bed, there are some uncertainties, and simplifications are needed to make the modeling possible. To justify the simplifications or to study the sensitivities of key parameters, some numerical studies are successfully done to investigate the influence of biomass properties (e.g., moisture content, particle size, density, solid conductivity, and heating value) and of process parameters (e.g., heat and mass transfer rates, bed porosity, devolatilization rate, PA flow rate, and heat capacity of both the gas and the solid phases) on the conversion rate, temperature, and gas compositions.<sup>31-36</sup>

(27) Kim, S.; Shin, D.; Choi, S. *Combust. Flame* **1996**, *106*, 241-251.  
 (28) Stubenberger, G.; Scharler, R.; Zahirovic, S.; Obernberger, I. *Fuel* **2008**, *87*, 793-806.  
 (29) Weissinger, A.; Fleckl, T.; Obernberger, I. *Combust. Flame* **2004**, *137*, 403-417.  
 (30) Kær, S. K. *Fuel* **2004**, *83*, 1183-1190.  
 (31) Johansson, R.; Thunman, H.; Leckner, Bo. *Energy Fuels* **2007**, *21*, 1493-1503.  
 (32) Shin, D.; Choi, S. *Combust. Flame* **2000**, *121*, 167-180.  
 (33) Thunman, H.; Leckner, B. *Proc. Combust. Inst.* **2005**, *30*, 2939-2946.  
 (34) Yang, Y. B.; Sharifi, V. N.; Swithenbank, J. *Fuel* **2004**, *83*, 1553-1562.



(a) Gas species at the fuel bed top



(b) Velocity and temperature at the bed top

Figure 5. Output of Bed Model-II.

Table 2. Examples of Adjusted A and B in the ED Model

study subject	new A	new B	adjusted by	reference
swirling pulverized-coal (PC) flame	0.5-0.7		the best flame prediction	38
fiberboard/wood chips fired traveling grate	0.6		the best agreement between the measured and the predicted CO	39
IFRF swirling PC furnace	0.6	10 <sup>20</sup>	the best prediction results	37
straw-fired vibrating grate	1		matching available CO	25

In principle, the third approach is similar to the first one: the first one is commercial code-based while the third one is in-house code developed by different researchers. Here, the second and the third approaches are used to investigate the effect of bed models in grate boiler simulations.

(1) Bed Model-I: on the basis of the experience and the design of this grate boiler, the biomass conversion rate is prescribed as a function of the position on the grate, as shown in Figure 3. Then, the inlet conditions of the combustion gas released from the fuel bed into the freeboard can be calculated from the overall heat and mass balances of the biomass, PA, and incident radiation heat flux. Figure 4 shows the calculated profile of gas species, velocity, and temperature at the fuel bed top.

(2) Bed Model-II: it is a one-dimensional transient fixed-bed model. The transport equations are solved for the gas and particle phases, separately. Submodels (e.g., evaporation, pyrolysis, combustion of volatiles, and char oxidation) are

(35) Yang, Y. B.; Ryu, C.; Khor, A.; Yates, N. E.; Sharifi, V. N.; Swithenbank, J. *Fuel* **2005**, *84*, 2116-2130.  
 (36) Zhou, H.; Jensen, A. D.; Glarborg, P.; Jensen, P. A.; Kavaliuskas, A. *Fuel* **2005**, *84*, 389-403.

Table 3. Cases Used for the Sensitivity Analysis

	case 1	case 2	case 3	case 4	case 5
grid	Mesh-I	Mesh-II	Mesh-I	Mesh-I	Mesh-I
bed model	Bed Model-I	Bed Model-I	Bed Model-II	Bed Model-I	Bed Model-I
turbulence model	SKE	SKE	SKE	RKE	SKE
constant $A$ in ED	default	default	default	default	$A = 0.6$
gas combustion	finite rate/ED (with default $B$ ); a two-step reaction with CO as intermediate species				
radiation	discrete ordinates model; domain-based WSGGM for absorption coefficient				
superheaters (SH)	SH-2 and SH-3 are modeled as slabs of fixed temperatures; SH-1 and ECO2: porous zones				
biomass particles	no particles entrained into freeboard				

solved for the source terms in the transport equations. Empirical correlations are used to calculate, for example, physical properties, chemical reaction rates, mixing rates, and heat transfer between the two phases. The time elapsed since ignition is mapped to the horizontal position on the grate by the bed moving speed. The model is partly validated by the experimental data from a laboratory-scale fixed-bed test rig. All the details about the governing equations, properties, submodels, and kinetics, as well as the sensitivities of some parameters, are given and explained in ref 36. Here, it is used to provide another profile of gas species, velocity, and temperature at the bed top, as shown in Figure 5.

As seen in Figure 5, the temperature peak predicted by Bed Model-II could be too high. However, the main concern here is not to conclude how accurate the bed models are. Instead, Bed Model-II is used in this paper just to provide different grate inlet conditions for the sensitivity analysis and to examine how significantly the bed models will affect the overall CFD results of the grate boiler.

**On Turbulence Models.** The standard  $k-\varepsilon$  (SKE) model is the most widely used turbulence model in industrial applications. However, it has some deficiencies; for instance, it cannot guarantee the positivity of normal stresses or Schwarz's inequality of shear stresses.<sup>37</sup> For the SKE model, the normal stress will be negative (i.e.,  $\overline{u'^2} < 0$ ) in flows with high strain rates, which is of course unphysical,

$$\frac{k}{\varepsilon} \frac{\partial U}{\partial x} > \frac{1}{3C_\mu} = \frac{1}{3 \times 0.09} \approx 3.7 \quad (2)$$

where  $k$ ,  $\varepsilon$ ,  $C_\mu$ , and  $\partial U/\partial x$  represent turbulent kinetic energy, energy dissipation rate, SKE model constant, and velocity gradient, respectively.

A realizable  $k-\varepsilon$  (RKE) model is developed to address the deficiencies of the SKE model. The RKE model generally has a better performance than the SKE model. In industrial boilers, zones of large strain rates are normally demanded by design to improve mixing and combustion. Therefore, the RKE model is expected to produce a better solution.

**On Combustion Models.** Finite rate/eddy dissipation (ED) using a two-step reaction with CO as the intermediate species is employed here as the combustion model. For this model, overpredicted flame temperature peak is an inherent problem for the following reasons: (1) The chemistry is described only by a two-step global mechanism without accounting for the intermediate species or the dissociation effects that occur at high temperatures. The chemical heat tied up in chemical bonds will be released as sensible heat. Therefore, the flame temperature is most likely to be overpredicted. (2) The default values for the  $A$  and  $B$  constants in the ED model could be too aggressively set. There is no theoretical background for the default values ( $A = 4$  and  $B = 0.5$ ) to be valid for general applications. Effects of the two constants in the ED model are studied here.

For 1 kg Fuel +  $r_f$  kg Oxidizer =  $(1 + r_f)$  kg Product, the fuel combustion rate in  $\text{kg}/(\text{m}^3 \cdot \text{s})$  calculated by the ED model is

$$R_{\text{comb}} = \min \left( A \rho_k^\varepsilon Y_F, A \rho_k^\varepsilon \frac{Y_{\text{Ox}}}{r_f}, AB \rho_k^\varepsilon \frac{Y_{\text{Pr}}}{1 + r_f} \right) \quad (3)$$

where  $Y_F$ ,  $Y_{\text{Ox}}$ , and  $Y_{\text{Pr}}$  represent the mass fraction of fuel, oxidizer, and product, respectively. The reaction heat, proportional to the combustion rate, is an important source in the energy equation. So, the calculated flame temperature peak could be tuned down by reducing the constant  $A$  in the ED model. In this paper, the constant  $A$  is adjusted by matching the calculated temperature peak to the measurements and the observation. Table 2 just gives a few references in which different values of the constant  $A$  or  $B$  are used and by what criteria the constant is adjusted.

**Summary of Sensitivity Analysis Results.** Table 3 summarizes some of the cases, which are done for the sensitivity analysis.

Figures 6–8 show the results of cases 1–3 at the same representative plane between the two side walls, respectively. The calculated temperature peaks in case 1 and case 2 are nearly the same, about 2266 K. The temperature peak in case 3, about 3057 K which is from the output of Bed Model-II (see Figure 5), exists at the bed top. Here, the same temperature range is used to ease the comparison.

The effect of meshes can be seen by comparing Figures 6 and 7. The only difference between the two cases is the mesh. Different mesh schemes lead to significant differences in the CFD results in the freeboard: the flow patterns are quite different, as well as the temperature and species distributions. Mesh quality affects face-flux calculations between cells and therefore directly impacts the accuracy of the solution and the convergence. Besides the grid quality, grid density also plays an important role since it determines how densely the discrete solutions are used to approximate the continuous solutions. A mesh of high grid density and quality always tends to improve the accuracy of CFD results.

The effect of bed models can be seen from Figures 6 and 8. The only difference between the two cases is the bed model, that is, the grate inlet conditions. The comparison may indicate that the bed models do not make as significant differences in the overall results as the meshes. Big differences in the vicinity of the bed can be observed as a result of the different grate inlet conditions. However, the differences are virtually restricted to the vicinity of the fuel bed. The flow pattern and even the temperature distribution in the majority of the furnace volume

(37) Fluent Inc. Lecture notes on Advanced Combustion Modeling in Fluent; Fluent User Services Center, 2005.

(38) Visser, B. M. PhD Thesis, TU Delft, Delft, The Netherlands, 1991.

(39) Scharler, R.; Fleckl, T.; Obernberger, I. *Prog. Comput. Fluid Dyn.* **2003**, *3*, 102–111.

(40) Bak, J.; Clausen, S. *Meas. Sci. Technol.* **2002**, *13*, 150–156.

(41) Clausen, S.; Bak, J. *Meas. Sci. Technol.* **2002**, *13*, 1223–1229.

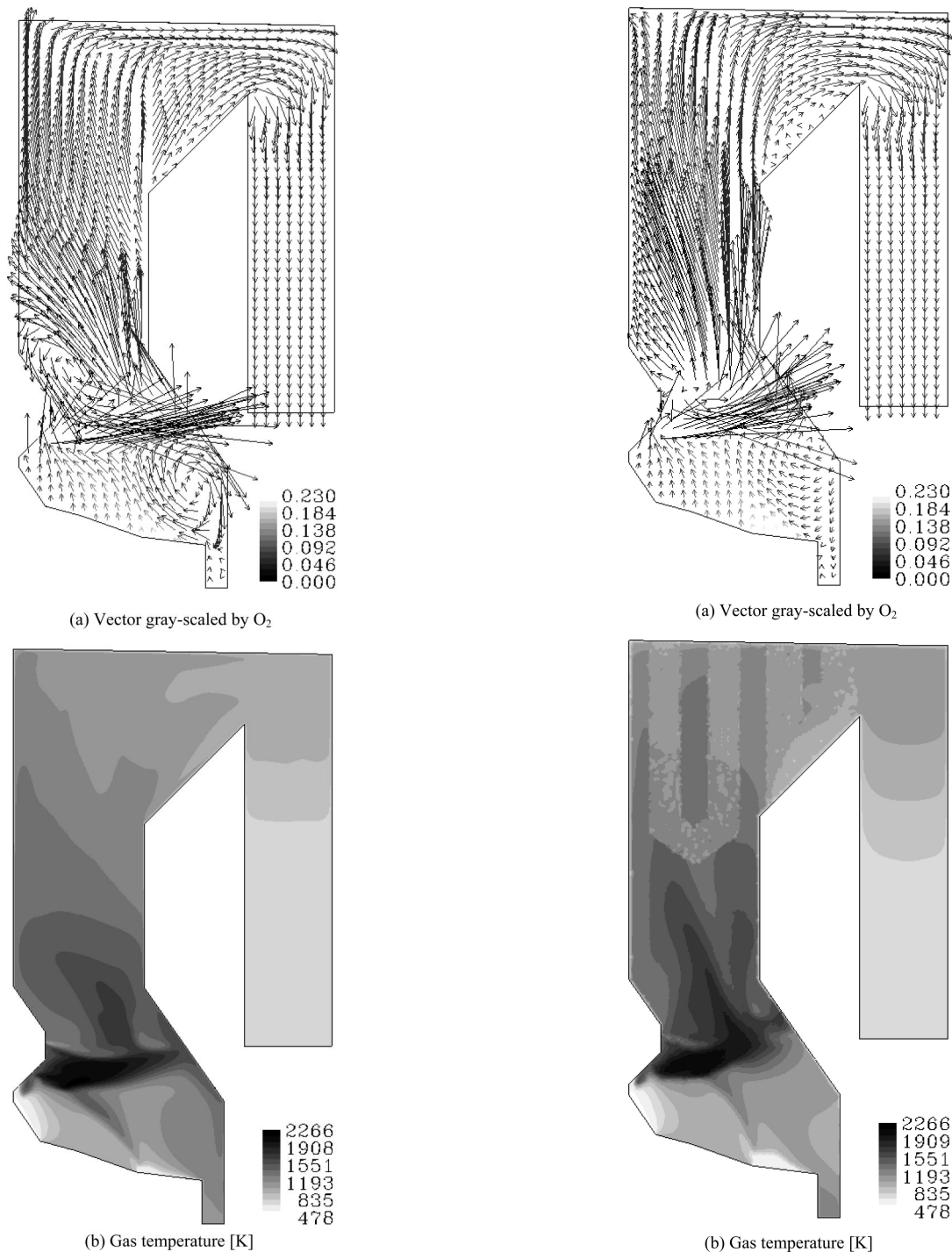


Figure 6. Results of case 1.

Figure 7. Results of case 2.

are still similar in the two cases. This could be attributed to the large amounts of air jets of high velocity, which affect significantly the mixing and combustion patterns in the freeboard.

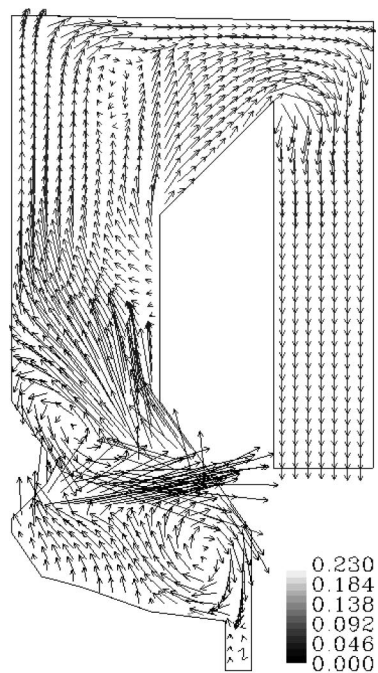
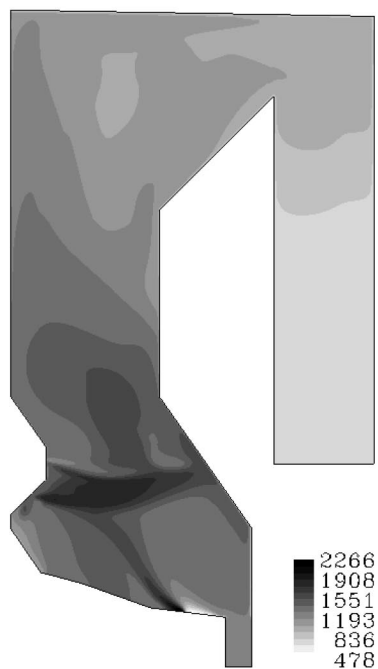
The detailed CFD results of other cases are not shown here. From the sensitivity analysis, the following conclusions could be drawn.

(1) The mesh is one of the most important factors in CFD modeling. To achieve reliable CFD results, a mesh of high density and high quality is preferred. A good mesh should be able to adequately resolve the geometric features, as well as the main flow physics in the geometry. Mesh-I is employed to establish the baseline CFD model.

(2) The bed model plays an important role in modeling of grate boilers. It provides the grate inlet conditions for the

freeboard modeling. Chemical reactions in the freeboard may be quite sensitive to the grate inlet conditions. However, in terms of the overall flow pattern and temperature distribution in the freeboard, the bed model might not be as important as the mesh: Its main influence is restricted to the vicinity of the fuel bed. Experience- or measurements-based bed models have been proven quite robust and useful in studying biomass combustion in industrial grate boilers, for instance, in the recent works.<sup>7,11,15</sup> Moreover, the noncontinuous biomass feeding and the combustion instabilities inside the fuel bed, as well as the uncertainties with the grate movement and the fuel bed properties, make it hard to derive a reliable and robust bed model. In this study, Bed Model-I is used to define the baseline CFD model.



(a) Vector gray-scaled by O<sub>2</sub>

(b) Gas temperature [K]

**Figure 8.** Results of case 3.

(3) Turbulence models make some differences in the CFD results but not as significantly as the mesh and bed model. RKE is the favorite model in the simulation of a combustor in which recirculation zones exist. RKE is used in the baseline CFD model in this study, while SKE is only used for a reference.

(4) Different values of the constant  $A$  in the ED model give rise to some differences in the calculated gas temperatures as a result of the different reaction rates determined by eq 3. Using the ED model with the default constants  $A$  and  $B$  results in a too high flame peak in this freeboard, about 2266 K as seen in Figures 6 and 7. By adjusting  $A$  to 0.6, the flame peak can be

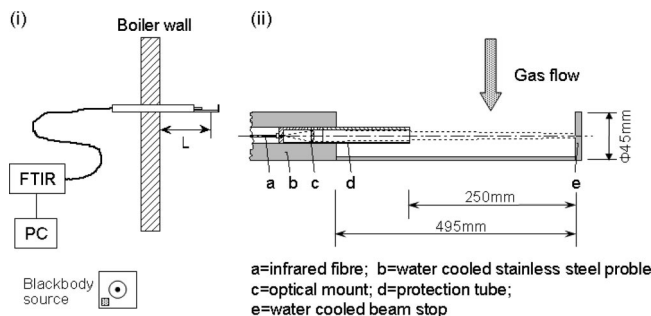


**Figure 9.** (i) FTIR measurement probe connected to an FTIR spectrometer, with the measurement distance,  $L$ , defined; (ii) a cross-sectional view of the probe head. The arrow illustrates the desired gas flow direction with minimum disturbance.

reduced to about 2000 K, which is more reasonable for such a biomass-fired grate boiler.

### Experimental Study

Compared with the modeling efforts, there are few experimental works in the literature that study the mixing, combustion, and deposition in full-scale industrial biomass-fired grate boilers.

In this work, the gas temperature and concentrations (H<sub>2</sub>O, CO, CO<sub>2</sub>) are measured simultaneously using a fiber optic probe connected to a Fourier transform infrared (FTIR) spectrometer. The experimental setup and a close-up view of the probe head are shown in Figure 9. First, the gas temperature is found by simple means from the CO<sub>2</sub> band at 2300 cm<sup>-1</sup>. Usually the CO<sub>2</sub> concentration in flue gas drops in the range from 8% (for gas combustion) to 13% (for coal combustion), which leads to errors in the temperature measurement less than 3.4 at 800 °C. Then, the transmittance spectra are calculated knowing the gas temperature and correcting for the background. The gas concentrations (H<sub>2</sub>O, CO, CO<sub>2</sub>) are determined by comparing the transmittance spectra with a spectroscopic database and validation measurements using the Hotgas facility. The accuracy of the measured H<sub>2</sub>O concentration can be improved by replacing the Hitemp database with the measured spectra from the hot gas cell. Better quality H<sub>2</sub>O reference spectra will also give rise to more accurate CO<sub>2</sub> and CO measurements as a result of the overlapping H<sub>2</sub>O lines. The details of this measuring technique can be seen in refs 40 and 41.

In this paper, the measured gas temperature and water vapor volume fraction are used for CFD validation because they are among those determined first from the measured raw data and may have less errors.

### Baseline CFD Model: Results and Discussion

On the basis of the above sensitivity analysis and the two-day measuring campaign, a baseline CFD model is defined for 100% load. The main data of the boiler (e.g., water, steam, biomass, air, and flue gas) are given in Table 4. Figure 10 shows the final output of the bed model after several switches between the bed model and the freeboard CFD modeling.

**Calibration of the Baseline Model.** Table 5 shows part of the calibration results for the baseline CFD model. The expected values in the table are either directly from or calculated from the plant control system data. The overall heat balance is also checked for the baseline results. The calibration results are quite satisfactory. Then, the CFD results are compared to the measured data.

**Validation of the Baseline Results.** Figure 11 shows part of the validation results, where the baseline results are compared against the FTIR measurements at a few representative ports. Here, Port K (center) and Port K (right) represent the port just at the center between the two side walls and the port close to



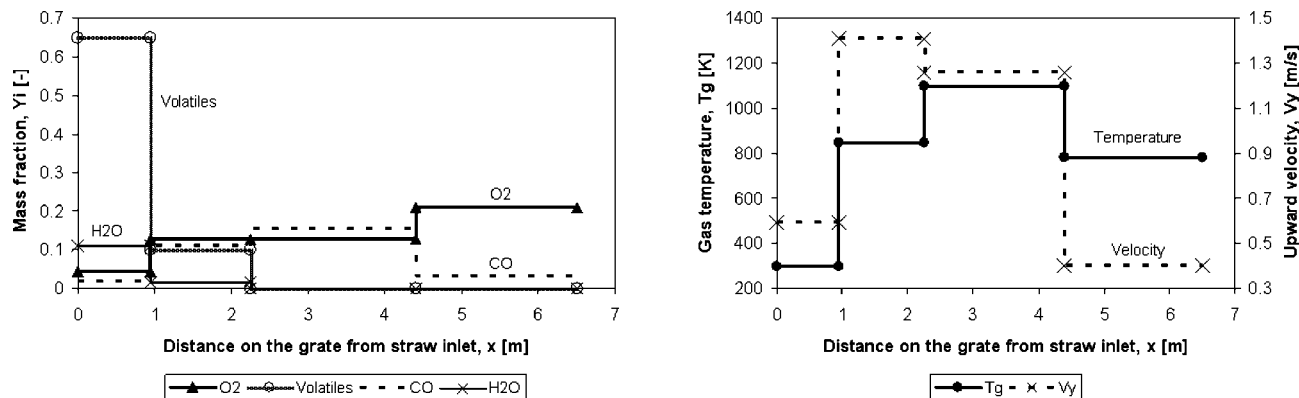


Figure 10. Final grate inlet conditions used in the baseline CFD model.

Table 4. Main Data of the Biomass-Fired Grate Boiler at 100% Load

data of water, steam, air, and flue gas		data of biomass (wheat straw) fired			
feed water temperature [°C]	170	feeding rate [kg/s]	7.14	ash [%, dry]	4.65
main steam Q [ton/h]/P [bar]/T [°C]	144/300/540	moisture [%, AR]	12	C [%, dry]	46.95
total PA/total SA [kg/s]	19.41/27.45	volatiles [%, dry]	79	H [%, dry]	6.1
PA and SA temperature [°C]	199	fixed carbon [%, dry]	16.35	N [%, dry]	0.435
gas temperature after air heater [°C]	165	LHV [MJ/kg, AR]	15.21	O [%, dry]	41.865

Table 5. Calibration of the Baseline CFD Results for 100% Load

terms	expected	CFD	overall heat balance check of CFD results	
heat at furnace rear wall [MW]	13.32	13.18	sensible heat from grate [MW]	4.42
heat at furnace side walls [MW]	9.14	9.46	chemical heat from grate [MW]	100.89
heat at furnace front wall [MW]	7.41	7.70	sensible heat of SA and OFA [MW]	4.87
heat at crossover and rear pass [MW]	5.55	5.23	heat by steam (incl. ECO2) [MW]	-78.08
heat at SH2 [MW]	15.79	15.82	heat carried by flue gas [MW]	-32.01
heat at SH3 [MW]	3.89	3.79	heat out of ash pit [MW]	-0.35
gas temperature after ECO2 [K]	824	822	overall heat imbalance [MW]	-0.26
O <sub>2</sub> fraction after ECO2 [vol %]	4.23	4.22	overall heat imbalance percentage	-0.2%

the right side wall, respectively (see Figure 1 for the elevation of Port K). Because the measuring volume is a slab of inhomogeneous gas at highly turbulent conditions over a 25 cm path, two gas temperatures are estimated from the measured spectra. One is the average temperature (labeled “Measured T”), and the other is the highest value detected over the 25 cm path (labeled “Measured T<sub>max</sub>”).

The validation shows or reveals the following issues:

(1) Differences exist between the SKE-based and the RKE-based results: the latter shows a better agreement with the measurements in the tendency than the former, as expected.

(2) At most of the measuring ports, the baseline results show an overall acceptable agreement with the measurements in both the gas temperature and the vapor fraction.

(3) However, relatively big discrepancies are still observed at a few measuring ports. Among all the ports, the largest discrepancy is found at port K (center), that is, in Figure 11c.

(4) The large discrepancies are thoroughly examined from both the modeling and the measuring sides. The errors from the modeling side could have been minimized through the efforts in the sensitivity analysis and the above calibration. The measurement technique is well validated, and the error from the measuring side could also play a minor role. For instance, the Hitemp database is currently used for the quantification for H<sub>2</sub>O in the flue gas, which may overestimate H<sub>2</sub>O and CO<sub>2</sub> concentrations to a limited extent.

(5) The discrepancies are believed to be mainly due to the boundary conditions used in the baseline CFD model. Some of the boundary conditions are quite hard to determine for a biomass-fired grate boiler in operation and could be very different from the real conditions for some reasons, for instance, (1) noncontinuous feeding of biomass into the real boiler. The real feeding of biomass is far from being continuous and uniform while the modeling is based on the mean feeding rate averaged over the entire grate area during the measuring period. In the real boiler, the fuel feeding rates onto the two center lines could be bigger than those onto the two side lines, leading to higher gas temperatures at the center. This may explain why the measured temperatures at port K (center) are much higher than those predicted by the baseline model. Another reason is (2) combustion instabilities in the fuel bed. The instabilities are very common for grate boilers. Ten grate boilers from five manufacturing companies, using various types of fuel mixtures, have been visited and investigated for this issue.<sup>42</sup> In all except one of the ten furnaces, combustion disturbances are encountered. The most common disturbance in the inventory is local burnouts inside the fuel bed, that is, areas where the intensity of the combustion is higher than in the surrounding areas. The local burnouts could be responsible for the elevated emissions of pollutants and the increased material wear. The second common

(42) Hermansson, S.; Olausson, C.; Thunman, H.; Rönnback, M.; Leckner, B. *Proceedings of 7th European Conference on Industrial Furnaces and Boilers*, Porto, April 18–21, 2006; INFUB: Rio Tinto, 2006.

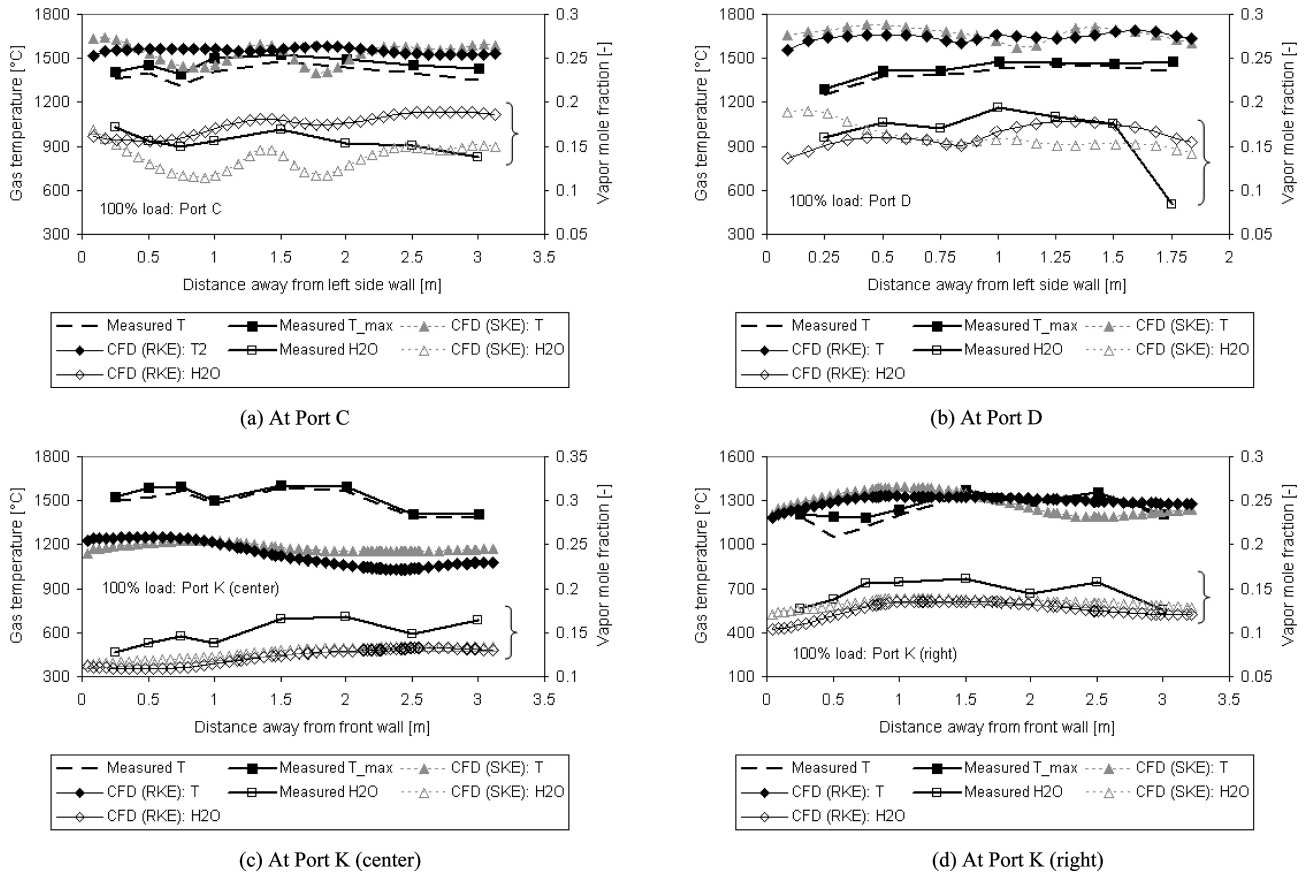


Figure 11. CFD results vs FTIR measurements at four of the measuring ports at 100% load.

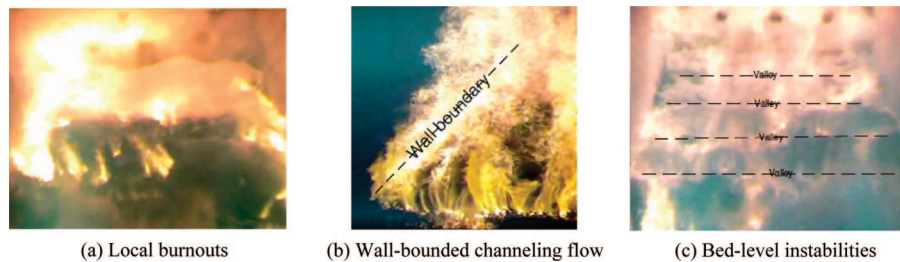


Figure 12. Three kinds of common combustion disturbances in fuel beds of grate furnaces.<sup>42</sup>

disturbance in the inventory is the channeling effect at the bounding furnace wall. The tendency to create burnouts and channeling is amplified by a spatially uneven fuel bed thickness. These combustion instabilities, as shown in Figure 12, also make it difficult to estimate reliable grate inlet conditions for the freeboard modeling. The last reason is (3) deposit formed on the furnace walls and the air nozzles. Deposition formation is another common problem in biomass-fired grate boilers. The pictures taken from this boiler (Figure 13) show the deposit formed on the rear wall and on the air nozzles in this furnace. The irregular deposit makes it hard or even impossible to define the precise wall and air-jets condition in the CFD modeling. In the baseline model, the air-jets orientation and momentum are determined from the designed values in a clean boiler, without considering any deviation due to the deposit at the nozzle exit.

The discrepancies between the baseline results and the measurements could be understood. Even though the discrepancies exist, the baseline model still captures the main mixing and combustion features in the boiler: the baseline results show an overall acceptable agreement with the measurements at most of the ports and the site observations.

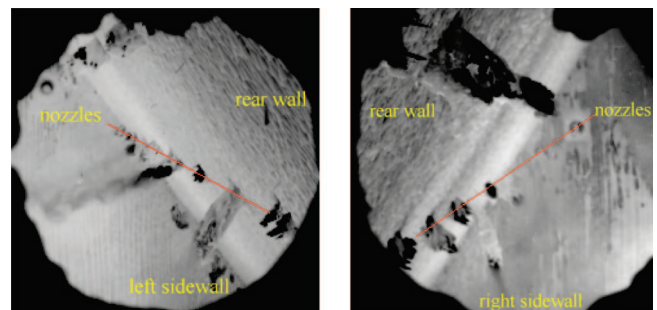


Figure 13. Deposit formed on the rear wall and on the air nozzles in this grate boiler.

**Discussion of the Baseline Results.** The baseline results on four representative cross sections are presented here.  $Z = 0.2125$  m is a vertical cross section near the center plane between two side walls;  $Z = 3.6125$  m is close to the plane where Port K (right) is located;  $Y = 8.075$  m is the horizontal cross section where Ports C and D lie;  $Y = 10.1$  m is the section where the OFA nozzles are located. See Figure 3s in the Supporting Information for a better view of these cross sections in the grate boiler.

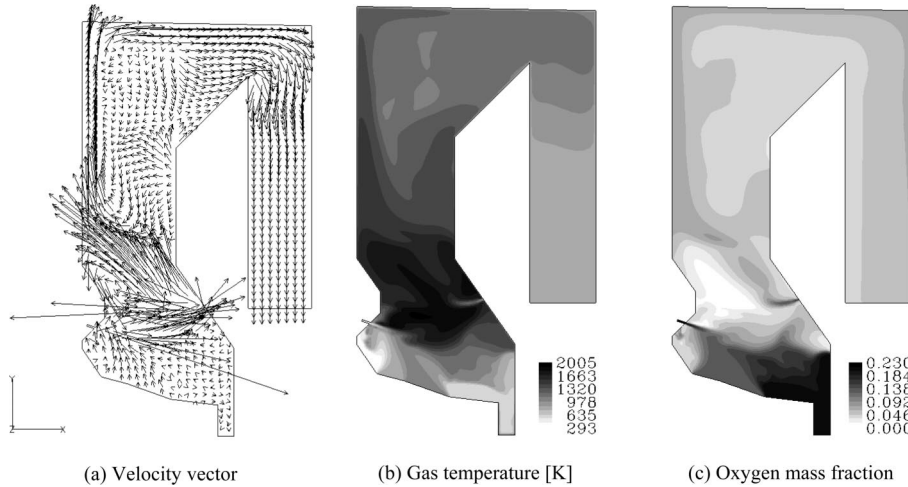


Figure 14. Baseline CFD results at Z = 0.2125 m.

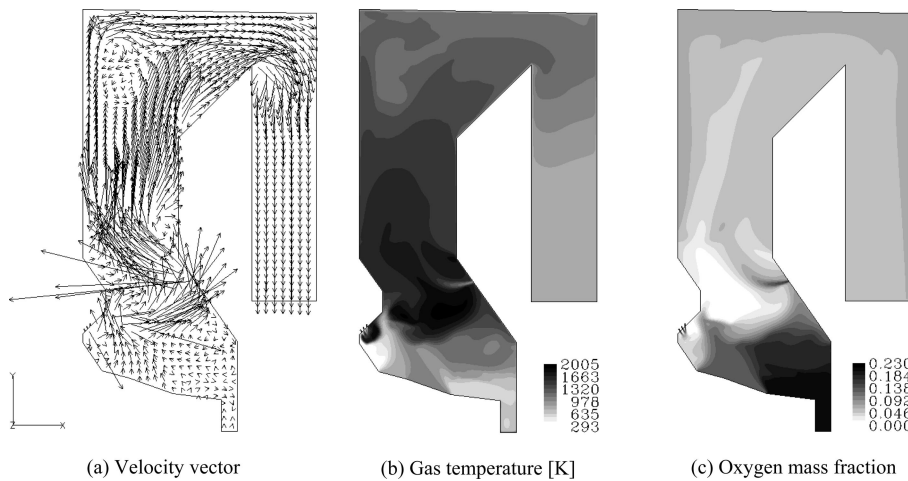


Figure 15. Baseline CFD results at Z = 3.6125 m.

Figures 14 and 15 show the flow, temperature, and oxygen distribution on the two vertical cross sections, respectively. Mixing is always important for combustors. The results show that the overall mixing in the design boiler is acceptable. Too large a recirculation zone on the vertical planes is not observed in the radiation pass of the design boiler, which usually makes the main flow of combustion gas confined into a high-speed narrow stream, shortens the residence time of combustible gas, worsens the mixing, and finally degrades the performance of the boiler. The mixing in the primary combustion zone is good as a result of the reasonable design of the local furnace geometry and the large amounts of air jets. The results indicate some small local recirculation zones in the vertical planes, which can improve local mixing. The existence of a high-speed, high-O<sub>2</sub> gas stream along the front wall, produced by the baseline model, shown in Figures 14c and 15c, is well confirmed by the measurements and site observations. The existence of such a stream is not good for the mixing and combustion in the burnout zone.

Figure 16 shows the velocity, gas temperature, mass fraction of oxygen, and volume fraction of water vapor on the two horizontal cross sections in the boiler. Rotating flows on horizontal sections are highly desired: they can enhance mixing, increase the residence time of the combustibles in the burnout zone, make the temperature distribution uniform, and create good burnout. The stronger the rotating flow is, the slower the rotation will decay in the radiation pass and the better the burnout performance will be. The spacing, momentum, and

arrangement of the air jets are very important for improving the mixing and combustion in the furnace. Too small a spacing between adjacent air jets will make them affected by each other and deteriorate the mixing. The results on plane Y = 8.075 m indicates that the jet spacing may be reasonable but that the jet momentum seems weak. Fewer but stronger jets could sometimes result in a better mixing than more but weaker jets. The OFA nozzle arrangement used in this boiler is favorable for enhancing mixing because the staggered OFA jets tend to create a double rotating flow on the horizontal cross section. However, Figure 16 e shows that the double rotating flow on this cross section is not as strong as designed, which implies that the spacing and the momentum of the OFA jets in the boiler could be optimized.

### Conclusions

A significant effort, in both modeling and experimentation, has been made toward a reliable baseline CFD model for a 108MW<sub>th</sub> biomass-fired grate boiler, which can be used for diagnosis and optimization of this boiler and design of new grate boilers. The following conclusions can be drawn from this study.

(1) Gas temperature and composition in biomass-fired boilers can be measured optically with an FTIR fiber optic probe. The available measuring ports restrict the zones in the boiler that can be mapped. The experimental setup needs to be extended for the measurements of O<sub>2</sub> (as well as NO and SO<sub>2</sub>) by using UV spectroscopy, since oxygen cannot be detected by FTIR.



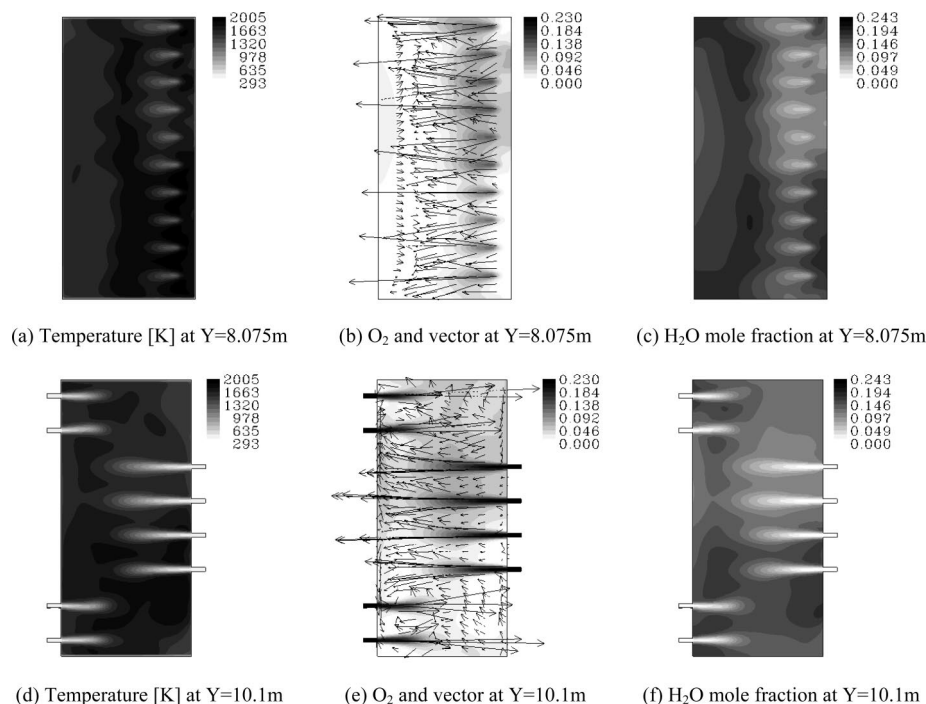


**Figure 16.** Baseline results at  $Y = 8.075$  and  $Y = 10.1$  m, respectively.

(2) The reliability of the baseline CFD model depends largely on the quality of the raw input data, the mesh, and the models, as well as the numerical methods, all of which should be correctly accounted for. The sensitivity analysis based on the design conditions indicates that the meshes, models for the fuel bed, turbulence, and combustion, discretization schemes, and inlet diffusion all play important roles in CFD modeling of grate boilers, among which the mesh could play an even more important role than the bed model in terms of the overall mixing and combustion patterns in the freeboard. The comparison between the baseline CFD model and the measurements reveals that the raw input data might be the main challenge in establishing a reliable baseline model for biomass-fired grate boilers, as a result of the large uncertainties in the biomass feeding and grate movement, the process parameters and physical properties of the biomass bed on the grate, the combustion instabilities inside the fuel bed, and the deposit formed on the walls and the air nozzles.

(3) At a few ports, large discrepancies between the baseline results and the measurements are observed, mainly as a result of the differences between the boundary conditions used in the simulations and the real conditions in the boiler. Nevertheless, the baseline model still shows an overall acceptable agreement with the measurements and the site observations. The overall mixing in the boiler is good: too large a recirculation zone is not observed on the vertical cross sections in the radiation pass. However, the mixing could be further improved by optimization of the air jets (e.g., the spacing, arrangement, location, momentum, and even the split of SA/PA), as well as the local arches of the boiler. The high-speed, high-oxygen gas stream along the front wall in the current boiler should be attenuated. A stronger double rotating flow should be enhanced on horizontal cross sections in the burnout zone. Preliminary optimizations are to be done on the basis of the baseline model.

(4) More efforts are needed in both the modeling and the experimentation. First, advanced monitoring and testing are needed to provide the modeling with the reliable inputs, for example, the biomass feeding and grate movement characteristics, the process parameters and physical properties of the biomass bed on the grate, the air jets, and the wall conditions, as well as the effects of deposit on them. Second, a more robust and reliable bed model is yet to be developed, for instance, by considering the transient features of the biomass feeding and grate movement, by accounting for the key instabilities in the fuel bed, by checking the species and energy balance, by including the necessary chemistry (e.g., N- or Cl-related reactions), and by a sensitivity analysis of the uncertainties with the bed model to derive a simplified, robust, and reliable bed model. Third, the CFD modeling needs to be extended to other topics of interest (e.g., dioxin/furan emissions) once the fundamental combustion chemistry knowledge is gained.

**Acknowledgment.** This work was financially supported by Grant PSO 4792, "Grate firing of biomass - Measurements, validation and demonstration". The authors would like to thank other project partners, P. Glarborg, H. Zhou, and P. A. Jensen from Technical University of Denmark, T. V. Jensen, E. Larsen, M. Kildsig, and B. Sander from DONG Energy, and K. Jørgensen from Babcock & Wilcox Vølund, for their helpful discussions during all the project meetings.

**Supporting Information Available:** Figures showing a clear view of the different processes in the biomass-fired grate boiler, local close-up of Mesh-I, and indications of the four cross sections. This material is available free of charge via the Internet at <http://pubs.acs.org>.

EF700689R